Interacting synapses stabilise both learning and neuronal dynamics in biological networks

Everton J. Agnes[1,2,*] and **Tim P. Vogels**[1,3]

[1]*Centre for Neural Circuits and Behaviour, University of Oxford, OX1 3SR Oxford, United Kingdom*
[2]*Biozentrum, University of Basel, 4056 Basel, Switzerland*
[3]*Institute of Science and Technology Austria, 3400 Klosterneuburg, Austria*

Distinct synapses influence one another when they undergo changes, with unclear consequences for neuronal dynamics and function. Here we show that synapses can interact such that excitatory currents are naturally normalised and balanced by inhibitory inputs. This happens when classical spike-timing dependent synaptic plasticity rules are extended by additional mechanisms that incorporate the influence of neighbouring synaptic currents and regulate the amplitude of their efficacy changes accordingly. The resulting control of excitatory plasticity by inhibitory activation, and vice versa, gives rise to quick and long-lasting memories as seen experimentally in receptive field plasticity paradigms. In models with additional dendritic structure, we observe experimentally reported clustering of co-active synapses that depends on initial connectivity and morphology. Finally, in recurrent neuronal networks, rich and stable dynamics with high input sensitivity emerge, providing transient activity that resembles recordings from motor cortex. Our model provides a general framework for codependent plasticity that frames individual synaptic modifications in the context of population-wide changes, allowing us to connect micro-level physiology with network-wide phenomena.

The remarkable property of synapses to change – synaptic plasticity – is hypothesised to be the brain's fundamental learning mechanism, and it has generated a large body of theoretical and experimental work[1–3]. Based on Hebb's postulate and early experimental data, theories have focused on the idea that synapses change depending on the activity of its pre- and postsynaptic counterparts, constituting a strong locality constraint. However, experimental evidence[4–11] has pointed towards learning mechanisms that also act non-locally, taking into account the activity at multiple synapses and even network state, for both excitatory and inhibitory synapses.

Excitatory synaptic plasticity (ESP) has long been known to rely on intersynaptic cooperativity by way of elevated calcium concentrations from the activation of multiple presynaptic excitatory synapses[8–11]. Interestingly, GABAergic, inhibitory synaptic plasticity (ISP) has also been shown to depend on the activation of neighbouring excitatory synapses[4,5] and on the ratio of local excitatory and inhibitory currents (EI balance)[4]. Finally, inhibitory currents can affect ESP by flipping the direction of efficacy changes according to the absence or presence of inhibitory currents in the vicinity of the synapse[6,7]. Long-term potentiation (LTP) at excitatory synapses has also been shown to depend on the distance and timing between successive LTP induction of neighbouring excitatory synapses[12]. Based on this experimental evidence we introduce a novel model of *codependent* synaptic plasticity, which takes into account the direct interaction between different synapses during plasticity. Our model reproduces a wide range of experimental data on excitatory plasticity, receptive field plasticity of excitatory and inhibitory synapses, synaptic clustering based on morphology, and stabilisation of amplified dynamics in recurrent networks.

In our framework (Fig. 1A), a synapse changes according to a function $\phi(E, I; \text{PRE}, \text{POST})$, in which E and I describe the recent postsynaptic activation of nearby excitatory and inhibitory synapses, respectively. The activity of the synapse's own pre- and postsynaptic neurons are described by PRE and POST. We consider E and I to be variables that depend on input currents: calcium influx through N-methyl-D-aspartate (NMDA) channels for E, and chloride influx through γ-Aminobutyric acid type A (GABA_A) channels for I (see Supplementary Material; Supp. M.). At excitatory synapses, $\phi(E, I; \text{PRE}, \text{POST})$ changes synaptic efficacy similarly to classic Hebbian spike-timing dependent plasticity (STDP)[8,13] (Fig. 1Bi), but in addition, neighbouring excitatory activity modulates synaptic changes in accordance with experimental results. Specifically, the learning rate for the Hebbian-LTP term increases linearly with neighbouring excitatory inputs[8,9,11] while heterosynaptic plasticity decreases synaptic efficacies via a quadratic dependency on the excitatory inputs[14] (Fig. 1Bii), counterbalancing the potentially de-stabilising positive feedback from Hebbian-LTP. Elevated inhibitory activity blocks excitatory plasticity[15], but allows for quick learning when the system undergoes disinhibition (Fig. 1Biii). Inhibitory synapses change according to a symmetric STDP curve[4,16] (Fig. 1Ci), but their learning-rate is modulated by the ratio of neighbouring excitatory and inhibitory activity (Fig. 1Cii,Ciii), such that when E and I currents are equal ($E = I$), or $E = 0$[4,5], there is no change in efficacy.

We tested the interplay between spike times and input currents through $\phi(E, I; \text{PRE}, \text{POST})$ in a leaky integrate-and-fire (LIF) neuron with plastic excitatory (AMPA and NMDA) synapses, as well as inhibitory (GABA_A) synapses (Supp. M.). We were able to capture many excitatory plasticity features, e.g., dependency on both the membrane potential depolarisation (Fig. 1D, left) and the frequency of pre- and postsynaptic spike pairs (Fig. 1D, right). In our model, high-frequency of pre- and postsynaptic spike pairs elicited increased LTP due to a direct elevation in NMDA currents, unlike spike-[19] or voltage-based[20] models that emulate this effect by detecting an increase in the postsynaptic firing frequency (Supp. M.). The explicit regulation of plasticity via excitatory and inhibitory currents highlights the different roles of excitation and inhibition for plasticity, which are inseparable in typical spike- or voltage-based learning rules (Supp. M.). Additionally, the positive feedback mechanism of Hebbian-LTP[17,21] is controlled by intrinsic heterosynaptic plasticity, creating a stable set-point for the excitatory currents (Fig. 1Bii, red circle). This set-point is determined by the ratio between heterosynaptic plasticity and Hebbian-LTP, independently of initial excitatory weights and inhibitory input strength (Fig. 1E). It acts as a normalisation

* Correspondence: everton.agnes@gmail.com;

1st April 2021

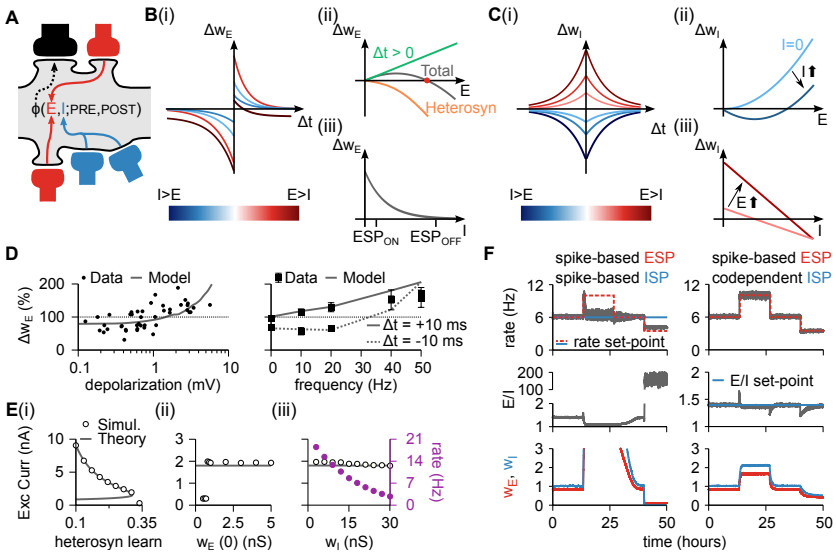

FIG. 1. Codependent synaptic plasticity normalises excitatory input and balances EI inputs. **A**, Plasticity of a synapse (black) depends on the activation of neighbouring excitatory (red) and inhibitory (blue) synapses. **B**, Codependent excitatory plasticity. (*i*), Excitatory weight change, Δw_E, is a function of the time interval between post and presynaptic spikes, Δt, and neighbouring synaptic inputs, E and I. (*ii*) Excitatory inputs, E, control Hebbian-LTP ($\Delta t > 0$) and heterosynaptic plasticity, creating a common fixed point for the total excitatory input (red dot). (*iii*), Inhibitory inputs, I, gate excitatory plasticity ('ON' *vs* 'OFF'). **C**, Codependent inhibitory plasticity. Inhibitory weight change, Δw_I, is a function of Δt (*i*), E (*Cii*) and I (*Ciii*) as in B. **D**, Fit of STDP experiments in mouse visual cortex for codependent excitatory plasticity, capturing observed voltage dependency[9] (left) and frequency dependency[8] (right) of synaptic changes. **E**, Total excitatory input (after learning) as a function of the ratio of the heterosynapic learning rate (*i*), initial excitatory weight (*ii*), and inhibitory weight (*iii*); inhibitory strength controls the postsynaptic neuron's firing-rate (*iii*; purple). **F**, Firing-rate (top), ratio between excitatory and inhibitory inputs (middle), and input weights normalised to initial value (bottom). Combination of excitatory[17] and inhibitory[18] spike-based rules (left); excitatory spike-based[17] and codependent inhibitory synaptic learning rules (right). Lines in the top panel indicate firing-rate fixed-points from excitatory (red) and inhibitory (blue) learning rules.

mechanism of excitatory inputs, resembling homeostatic regulation of excitatory bouton size in dendrites[22]. Importantly, inhibitory plasticity balances excitatory and inhibitory currents without imposing a firing-rate set-point, avoiding competition with excitatory plasticity (Fig. 1F).

To assess the functional consequence of codependent plasticity, we studied its performance in receptive fields formation for both excitatory and inhibitory synapses jointly[23]. We simulated a postsynaptic LIF neuron receiving inputs from 8 pathways (Supp. M.) that represent, e.g., different sound frequencies[18,23] (Fig. 2A). In this scenario, inhibitory activity acted as a gating mechanism for excitatory plasticity, by keeping the learning rate at a minimum when inhibitory currents were high (Fig. 1Biii). Excitatory input weights could thus only be changed during periods of presynaptic disinhibition, i.e., the learning window, and were otherwise stable[23] (Fig. 2B,C). Inhibitory weights, due to the spike-timing dependence of codependent ISP, precisely mirrored the excitatory receptive field after the learning window (Fig. 2D), a phenomenon known as detailed balance[3]. Changes in both excitatory and inhibitory inputs due to codependent plasticity robustly reproduced experimental results in rat auditory cortex[23] (Fig. 2E) without additional fine tuning.

Next, we attached passive dendritic compartments to the soma of our model to assess how our learning rules affected the dendritic organisation of synapses. Due to their largely passive properties, the membrane potential of dendrites could be depolarised to values above the somatic spiking threshold depending on their proximity, i.e., electrotonic distance, to the soma (Fig. 3A). Super-threshold membrane potential fluctuations gave rise to larger NMDA and $GABA_A$ current fluctuations in distal dendrites (Fig. 3B). When excitation and inhibition were unbalanced (i.e., when receiving uncorrelated inputs), distal dendrites could undergo fast changes due to the current-induced high learning rates for excitatory plasticity (Fig. 3B, thick red line). However, when currents were balanced (i.e., when receiving correlated excitatory and inhibitory inputs), large inhibitory currents gated excitatory plasticity off despite strong excitation, effectively blocking excitatory plasticity in these compartments (Fig. 3B, thick blue line). Additionally, the larger distance to the soma, and its consequently weaker passive coupling (Fig. 3C), meant that distal dendrites had smaller influence on the initiation of postsynaptic spikes.

As a consequence of these two effects – location dependent learning-rates and influence on spike initiation – synapses developed differently according to their somatic proximity (Fig. 3D), and according to the activity of their neighbouring inputs. When the majority of excitatory inputs onto a dendritic compartment were co-active (i.e., originated from the same source), co-active synapses were strengthened, creating a cluster of similarly tuned inputs onto a compartment. Independently active excitatory synapses weakened and eventually faded away (Fig. 3D, middle). In contrast, when more than a certain number of excitatory inputs were independent, co-active synapses decreased in weight and faded, while independently active excitatory synapses strengthened (Fig. 3D, right). The number of co-active excitatory synapses necessary for a dendritic compartment to develop single-feature tuning varied with somatic proximity, and whether excitation and inhibition were matched (Fig. 1E). Notably, in the balanced state, substantially more co-active excitatory synapses were necessary to create clusters for at distal than at proximal dendrites (Fig. 1E), because only large groups of co-active excitatory synapses could initiate (LTP-inducing) pre-before-post spike pairs. Thus, single-feature selectivity[25,26] or mixed selectivity[27] emerged in our model depending on the branch architecture of the dendritic host structure[28,29] (Fig. 3F).

Up to this point we explored the effects of codependent synaptic plasticity in a single postsynaptic neuron. However, the recurrent neuronal circuits typically amplify instabilities of any synaptic plasticity rules at play[17,21]. We thus investigated codependent plasticity in a recurrent neuronal network of 1250 spiking neurons (Supp. M.; Fig. 4A). In our model, excitatory and inhibitory codependent plasticity allowed the network to self-stabilise in a high-conductance state[30], with low effective neuronal membrane time-constants (Fig. 4C), and strong excitatory connections that were precisely balanced by equally strong inhibition (Fig. 4B). Further, the network exhibited a wide distribution of baseline firing-rates (Fig. 4D), similar to what has been observed in cortical recordings *in vivo*[31]. We analysed the final connectivity matrix of the net-

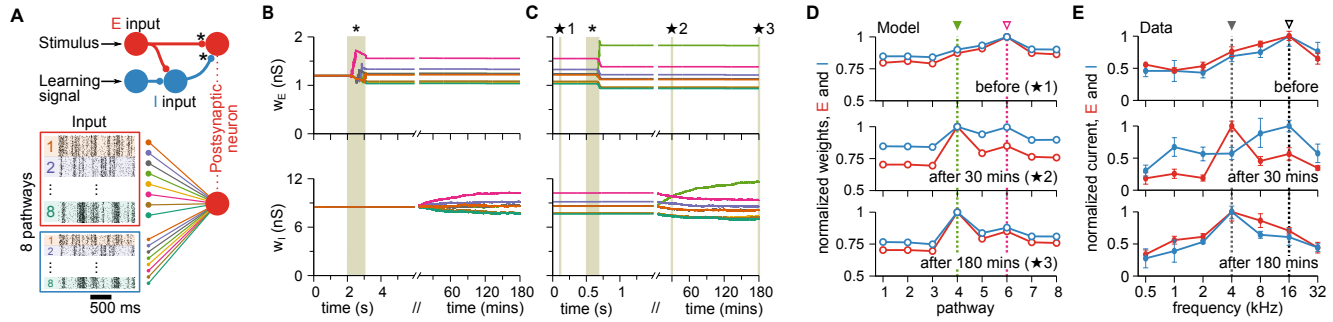

FIG. 2. Receptive field plasticity. **A**, External stimulus (e.g., sound) activates a set of correlated excitatory and inhibitory afferents (simulated as inhomogeneous Poisson point processes) that feed forward onto a postsynaptic neuron with plastic synapses (*). Eight group pathways, consisting of 100 excitatory and 25 inhibitory afferents each, have correlated spike trains. The responsiveness of inhibitory afferents can be modulated by an additional learning signal. **B**, Time course of excitatory (top) and inhibitory (bottom) weights (colour coded by groups). During a "learning window", indicated by the shaded area (*), all inhibitory afferents are down-regulated. The sequential activation of excitatory input groups in the absence of inhibition establishes a receptive field profile. **C**, Continued simulation from B. Weights are stable until inhibition is down-regulated for a 200-millisecond window (*), during which the green pathway (#4) is activated Consequently, the preferred input pathway switches from #6 (pink) to #4 (green). **D**, Snapshots of the average synaptic weights for the different pathways before (top), immediately after plasticity induction (middle), and at the end of the simulation as indicated by the ⋆ symbols in B. **E**, Experimental data[23] shows receptive field profiles of excitatory and inhibitory inputs before (top), as well as 30 minutes (middle) and 180 minutes (bottom) after pairing of non-preferred tone and nucleus basalis activation.

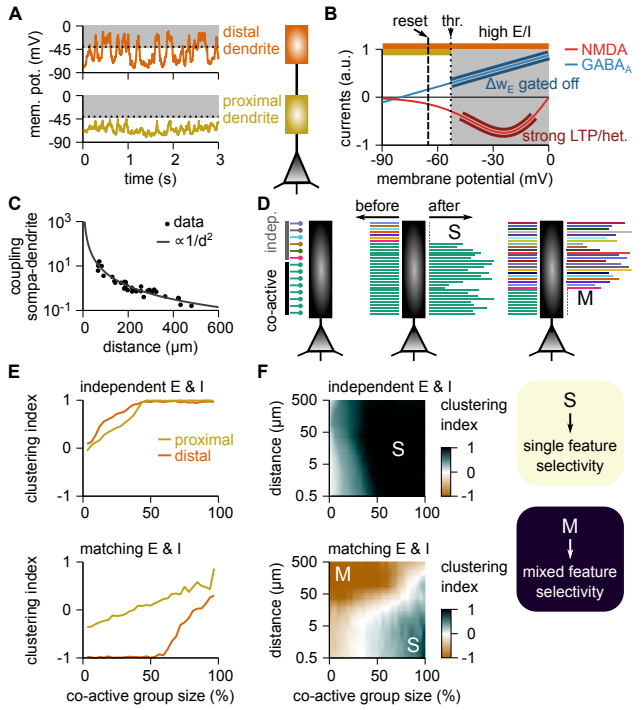

FIG. 3. Dendritic clustering. **A**, Membrane potential fluctuations at distal (top) and proximal (bottom) dendrites during ongoing stimulation. Dashed line shows the spiking threshold at the soma. **B**, NMDA (red) and $GABA_A$ (blue) currents as a function of membrane potential. Spiking threshold and reset are indicated by dotted and dashed lines, respectively. **C**, Coupling strength between soma and dendritic branch as a function of electrotonic distance fitted to experimental data[24]. **D**, *(Left)*, Schematic of the synaptic organisation onto a dendrite. Each line represents a synapse, with co-active synapses bearing the same colour. Examples of clustering of co-active (middle) or independent (right) synapses resulting in single feature selectivity (S) and mixed feature selectivity (M) at the level of the dendrite. Line length indicates synaptic weight in arbitrary units. **E**, Clustering index as a function to size of co-active input group for distal (orange) and proximal (yellow) dendrites with (top) or without (bottom) matching inhibitory inputs. Clustering index is equal to 1 (−1) when only co-active (independent) synapses survived and 0 all synapses surviving (Supp. M.). **F**, Same as E but showing dependency of distance between soma and dendritic branch.

work with regard to the weights of incoming and outgoing synapses to find the neurons would most strongly affect the network (Supp. M.; Fig. 4E). When we delivered step-like stimuli to these neurons. Their elevated firing rates maximally stimulated other neurons of the network, increasing or decreasing their responses based on the specific input pattern, and the network connectivity (Fig. 4F,G). We observed several types of responses, ranging from minimal deflections in firing rate to large transient responses, either during the delivery of the stimulus, or in response to its termination. To further quantify these responses, we calculated both the average and the ℓ_2-norm of the population (Fig. 4G). Both these measures confirmed that the network was in a regime of 'transient amplification' (Fig. 4G), i.e., a highly responsive state thought to underlie computation-through-population-dynamics[32]. What's more, the trajectory of the population dynamics in principle component space showed reliable network wide activity patterns (Fig. 4H) that could be used to control the activity of a readout network with two output units to draw digits (Fig. 4I).

In this paper we introduced a general framework to describe synaptic plasticity as a function of local pre- and postsynaptic interactions, including the modulatory effects of nearby synapses. We designed the excitatory and inhibitory plasticity rules according to experimental observations, such that the effect of neighbouring synapses gated, controlled and even flipped the direction of efficacy changes[4–12]. Importantly, excitatory and inhibitory plasticity strove towards different fixed points. They thus collaborated without mutual antagonism, in the process reproducing many relevant experimental results. In our model, inhibition played an important role to control excitatory plasticity, allowing for quick reorganisation of input patterns during periods of disinhibition, yet keeping memories stable when excitatory and inhibitory neurons were active. This control that inhibition exerted on excitatory plasticity also dictated whether co-active excitatory synapses clustered (or not) in a simplified dendritic model, providing a possible explanation for differing observations of dendritic input clustering in the recent literature[28,29]. Finally, our network results serve as a proof of principle that codependent plasticity can develop a stable, balanced network that amplify particular types of input, generating complex spatio-temporal patterns of

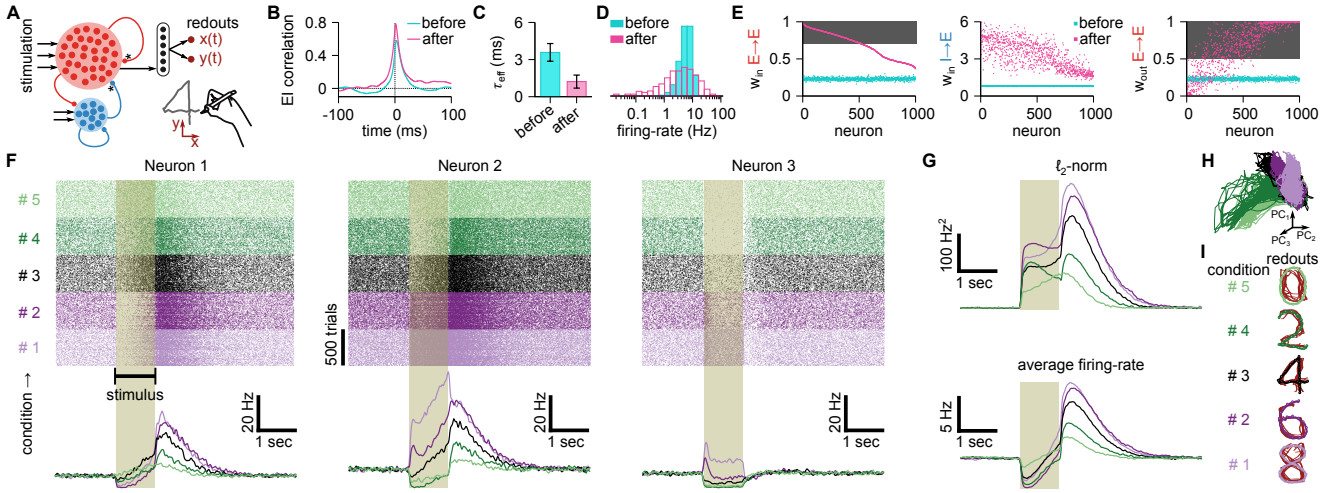

FIG. 4. Self-sustained activity and transient amplification in recurrent networks. A, Network of 1000 excitatory and 250 inhibitory neurons. Connections between excitatory neurons and from inhibitory to excitatory neurons are plastic (indicated by ∗). During learning external stimulation decreases over time until a state of self-sustained activity is reached. **B-E**, Summary of changes in excitatory neurons, before (cyan) and after (pink) a learning period of 60 minutes. **B**, Correlation between excitatory and inhibitory currents. **C**, Effective time constant, calculated as the membrane time constant divided by the sum of all conductances. **D**, Firing-rate distribution. **E**, Excitatory average input (left) and output (middle) weight, and inhibitory average weight (right) for all excitatory neurons, ordered by stronger input weights after learning. **F**, Raster plot (top) and mean firing-rate (bottom) of three excitatory neurons for five different stimulation patterns (conditions). **G**, Norm (top) and average firing-rate (bottom) of excitatory neurons for the five stimulation patterns in F. **H**, First three principal components of the activity of excitatory neurons from the recurrent network. Each line is the combination of 50 out of 500 trials to compensate for the high trial-to-trial variability (Supp. M.). **I**, Output of two readout neurons trained to draw digits on a 2D-plane using the input from the excitatory neurons from the recurrent network (Supp. M.).

activity. The networks that were constructed by codependent plasticity reproduced cortical activity patterns that were not trained for and could be used to emulate motor-like outputs for both average and single trial experiments[33,34]. Additional experimental work that can monitor multi-cell interactions by way of, e.g., all optical intervention *in vivo*[35,36] are necessary to help describe more complex synaptic interactions of multiple excitatory and inhibitory neuron types[37]. We are confident that codependence as a principle for plasticity will prove crucial in the face of increased complexity of these challenges.

Acknowledgements. We thank Chris Currin, Bill Podlaski, and the members of the Vogels group for fruitful discussions. This work was supported by a Research Project Grant by the Leverhulme Trust (RPG-2016-446; EJA), a Sir Henry Dale Fellowship by the Wellcome Trust and the Royal Society (WT100000; EJA, TPV), and a Wellcome Trust Senior Research Fellowship (214316/Z/18/Z; EJA, TPV).

References

[1] H. Markram, W. Gerstner, and P. J. Sjöström, Frontiers in Synaptic Neuroscience **3**, 4 (2011).
[2] M. Poo, M. Pignatelli, T. J. Ryan, S. Tonegawa, T. Bonhoeffer, K. C. Martin, A. Rudenko, L.-H. Tsai, R. W. Tsien, G. Fishell, C. Mullins, J. T. Gonçalves, M. Shtrahman, S. T. Johnston, F. H. Gage, Y. Dan, J. Long, G. Buzsáki, and C. Stevens, BMC Biology **14**, 40 (2016).
[3] G. Hennequin, E. J. Agnes, and T. P. Vogels, Annual Review of Neuroscience **40**, 557 (2017).
[4] J. A. D'amour and R. C. Froemke, Neuron **86**, 514 (2015).
[5] J. Mapelli, D. Gandolfi, A. Vilella, M. Zoli, and A. Bigiani, Proceedings of the National Academy of Sciences **113**, 9898 (2016).
[6] L. Wang and A. Maffei, Journal of Neuroscience **34**, 1083 (2014).
[7] V. Paille, E. Fino, K. Du, T. Morera-Herreras, S. Perez, J. H. Kotaleski, and L. Venance, Journal of Neuroscience **33**, 9353 (2013).
[8] P. J. Sjöström, G. G. Turrigiano, and S. B. Nelson, Neuron **32**, 1149 (2001).
[9] P. J. Sjöström and M. Häusser, Neuron **51**, 227 (2006).
[10] F. Brandalise, S. Carta, F. Helmchen, J. Lisman, and U. Gerber, Nature Communications **7**, 13480 (2016).
[11] D. Debanne, B. H. Gähwiler, and S. M. Thompson, Proceedings of the National Academy of Sciences **93**, 11225 (1996).
[12] C. D. Harvey and K. Svoboda, Nature **450**, 1195 (2007).
[13] G.-q. Bi and M.-m. Poo, Journal of Neuroscience **18**, 10464 (1998).
[14] M. Chistiakova and M. Volgushev, Experimental Brain Research **199**, 377 (2009).
[15] K. A. Wilmes, H. Sprekeler, and S. Schreiber, PLoS Computational Biology **12**, e1004768 (2016).
[16] M. A. Woodin, K. Ganguly, and M.-m. Poo, Neuron **39**, 807 (2003).
[17] F. Zenke, E. J. Agnes, and W. Gerstner, Nature Communications **6**, 6922 (2015).
[18] T. P. Vogels, H. Sprekeler, F. Zenke, C. Clopath, and W. Gerstner, Science **334**, 1569 (2011).
[19] J.-P. Pfister and W. Gerstner, Journal of Neuroscience **26**, 9673 (2006).
[20] C. Clopath, L. Büsing, E. Vasilaki, and W. Gerstner, Nature Neuroscience **13**, 344 (2010).
[21] A. Morrison, A. Aertsen, and M. Diesmann, Neural Computation **19**, 1437 (2007).
[22] T. Keck, G. B. Keller, R. I. Jacobsen, U. T. Eysel, T. Bonhoeffer, and M. Hübener, Neuron **80**, 327 (2013).
[23] R. C. Froemke, M. M. Merzenich, and C. E. Schreiner, Nature **450**, 425 (2007).
[24] A. T. Gulledge and G. J. Stuart, Journal of Neuroscience **23**, 11363 (2003).
[25] N. Takahashi, K. Kitamura, N. Matsuo, M. Mayford, M. Kano, N. Matsuki, and Y. Ikegaya, Science **335**, 353 (2012).
[26] D. E. Wilson, D. E. Whitney, B. Scholl, and D. Fitzpatrick, Nature Neuroscience **19**, 1003 (2016).
[27] H. Jia, N. L. Rochefort, X. Chen, and A. Konnerth, Nature **464**, 1307 (2010).
[28] T. Kleindienst, J. Winnubst, C. Roth-Alpermann, T. Bonhoeffer, and C. Lohmann, Neuron **72**, 1012 (2011).
[29] E. T. Kavalali, J. Klingauf, and R. W. Tsien, Proceedings of the National Academy of Sciences **96**, 12893 (1999).
[30] A. Destexhe, M. Rudolph, and D. Paré, Nature Reviews Neuroscience **4**, 739 (2003).
[31] K. B. Hengen, M. E. Lambo, S. D. Van Hooser, D. B. Katz, and G. G. Turrigiano, Neuron **80**, 335 (2013).
[32] S. Vyas, M. D. Golub, D. Sussillo, and K. V. Shenoy, Annual Review of Neuroscience **43**, 249 (2020).
[33] M. M. Churchland, M. Y. Byron, J. P. Cunningham, L. P. Sugrue, M. R. Cohen, G. S. Corrado, W. T. Newsome, A. M. Clark, P. Hosseini, B. B. Scott, D. C. Bradley, M. A. Smith, A. Kohn, J. A. Movshon, K. M. Armstrong, T. Moore, S. W. Chang, L. H. Snyder, S. G. Lisberger, N. J. Priebe, I. M. Finn, D. Ferster, S. I. Ryu, G. Santhanam, M. Sahani, and K. V. Shenoy, Nature Neuroscience **13**, 369 (2010).
[34] M. M. Churchland, J. P. Cunningham, M. T. Kaufman, J. D. Foster, P. Nuyujukian, S. I. Ryu, and K. V. Shenoy, Nature **487**, 51 (2012).
[35] A. M. Packer, L. E. Russell, H. W. P. Dalgleish, and M. Häusser, Nature Methods **12**, 140 (2015).
[36] M. B. Pardi, J. Vogenstahl, T. Dalmay, T. Spanò, D.-L. Pu, L. B. Naumann, F. Kretschmer, H. Sprekeler, and J. J. Letzkus, Science **370**, 844 (2020).
[37] X. Jiang, S. Shen, C. Cadwell, P. Berens, F. Sinz, A. Ecker, S. Patel, and A. Tolias, Science **350**, aac9462 (2015).